Available online at www.sciencedirect.com
ScienceDirect
Journal of Sound and Vibration 313 (2008) 308–324
JOURNAL OF SOUND AND VIBRATION
www.elsevier.com/locate/jsvi

Impact of mounting with an overlap on vibration and stability of a rotating annular plate

Ratko Maretic*, Valentin Glavardanov[1]

Faculty of Technical Sciences, University of Novi Sad, POB 55, 21121 Novi Sad, Serbia

Received 25 April 2007; received in revised form 14 November 2007; accepted 14 November 2007
Available online 27 December 2007

Abstract

In this paper, we investigate a thin annular plate, whose inner edge has a smaller radius before mounting onto a rigid shaft then the radius of the shaft itself. After mounting onto the shaft forcefully, the overlap appears on the plate where it touches the shaft. The plate spins together with the shaft at a constant angular speed. Two possible cases of supporting the outer edge of the plate have been examined—when the edge is clamped and when it is free. The paper presents the determined frequencies of small transversal vibration with respect to the size of the overlap and angular speed. When determining the frequencies, the Galerkin method has been used. Based on these data, plate stability was examined and the critical value of the angular speed was determined using the dynamic criterion. For the special case of a non-rotating plate, the critical value of the overlap at which the plate loses stability was determined.

Stability of a rotating plate with an overlap was also examined using nonlinear Karman's equations analysis applying the Ljapunov–Schmidt method. The analytical solution of the linearised equations system was obtained using the standard procedure. After that, the bifurcation equation was obtained and signs of the bifurcation coefficients were determined. Consequently, we came to the conclusions regarding the bifurcation type.

The conclusions of the bifurcation type have been corroborated by numerical integration of the differential equations system and certain stability loss cases have been presented on drawings.

1. Introduction

Rotating annular plates and discs are very frequently present as parts of transmission elements, pumps, compressors, circular saw blades, etc. This is why the need to investigate the vibration of these elements at various support and loading conditions has arisen. Determining the dynamic response of rotating discs, i.e. their shapes and natural frequencies, is the stepping stone in the design of rotating equipment. They are most commonly found in applications that contain bladed disc assemblies for turbines and flywheels.

The first analysis of rotating discs was performed by Lamb and Southwell [1]. It included determining the natural frequencies of a complete circular disc clamped at its centre and free at its edge. They applied power

*Corresponding author. Tel.: +381 214 852 239; fax: +381 214 58133.
E-mail addresses: maretic@uns.ns.ac.yu (R. Maretic), vanja@uns.ns.ac.yu (V. Glavardanov).
[1]Tel.: +381 214 852 251; fax: +381 214 58133.

0022-460X/$ - see front matter © 2007 Elsevier Ltd. All rights reserved.
doi:10.1016/j.jsv.2007.11.030

series techniques to determine the exact natural frequencies of a rotating membrane. Subsequently, they were then combined with previously published results for a non-rotating disc and the lowest natural frequency bounds for a rotating disc with both flexural and membrane effects present were determined. They also presented upper bounds for natural frequencies using Rayleigh's method. Southwell [2] later extended the results obtained earlier and included the case of a centrally clamped annulus under the assumption of partial clamping, He considered a disc constrained in the transverse but not in the radial direction at the hub. The results he obtained had approximate natural frequency calculations, which were later validated by Barasch and Chen [3]. The validation was performed using the modified Adams numerical method. Barasch and Chen [3] showed the nature of that influence in case of a rotating disc with the free edge, while Ramaian [4] showed the same in case of annular plates with various boundary conditions. The same technique was used by Eversman and Dodson [5] to obtain an exact series representation of the solution for a fully clamped rotating disc. Mote [6] examined the influence of initial and thermal membrane stresses on the vibration of circular saw blades. Schajer and Mote [7] investigated the influence of a special procedure that generates initial stresses in circular saw blades by using roll tensioning process. During the process the saw blade is compressed by two opposing rollers that make a plastically deformed annular zone on the saw blade. It is shown that this process leads to an increase in critical speed.

Maretic [8] proved that a rotating circular plate subjected to certain boundary conditions can lose stability under inertial load. Ouyang and Mottershead [9] analysed vibration and stability of a rotating car disc brake. For the case of the thick circular plate described by Karman's nonlinear plate theory stability analysis is given in Wolkowisky [10]. Stability of a clamped annular plate, which is descibed by Karman's nonlinear plate theory, is presented in Machinek and Troger [11]. In this paper, the Ljapunov–Schmidt method was used. Raju and Rao [12] presented stability analysis of a moderately thick circular plate. Maretic and Glavardanov [13] examined the stability of a heated rotating circular plate with elastic support.

When manufacturing constructs with rotating annular plates, the plate is sometimes mounted onto the shaft with an overlap. Before mounting the plate and when stationary, the plate radius of the inner edge is less than the shaft radius by a small value δ (Fig. 1a), which will be referred to as an overlap. It will be assumed that the shaft is ideally rigid. After forcing the shaft into the plate, the inner edge radius is changed and the stress appears in the plate. In this paper we shall look at two cases of supporting the plate: the first (Fig. 1b) when the plate outer edge is clamped to a rigid cylinder revolving axially with the plate, and the second (Fig. 1c) when the outer edge is free.

We note that the assumption on the shaft being ideally rigid makes this plate model is unacceptable in most practical cases since the elastic moduli of the shaft and the plate are usually of the same order of magnitude. However, there is a case where up to the same reasonable point our model can be acceptable from the physical

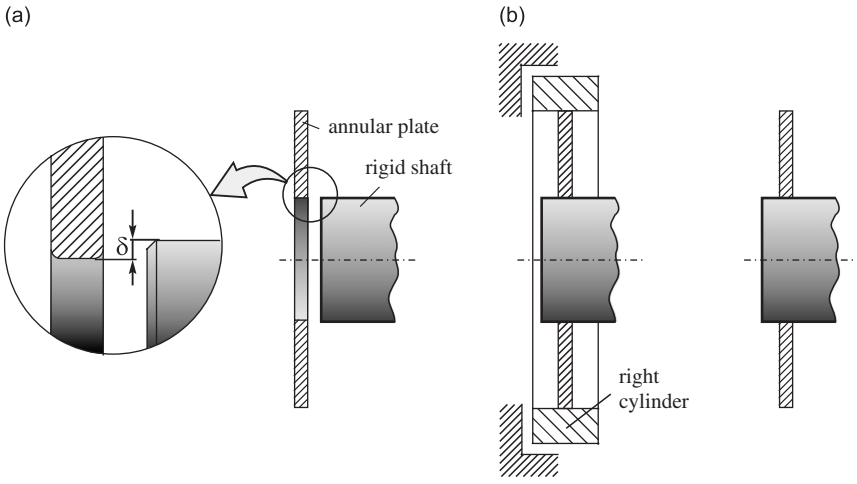

Fig. 1. The plate and shaft: (a) before mounting, (b) after mounting with an overlap—outer edge is clamped, and (c) after mounting with an overlap—outer edge is free.

point of view. This case, shown in Fig. 1c presents plate models of grinding wheels and sand paper wheels for polishing. These plates are made of materials having significantly smaller elastic moduli than steel used for the shaft. An overlap usually occurs as a consequence of mounting or as a consequence of mistakes in manufacturing. However, it can also be induced by thermal effects caused by unequal coefficients of thermal expansion of the plate and shaft.

This paper will look at what the impact of both the overlap and angular speed is on transverse vibration of the plate and its stability.

2. Mathematical formulation of the problem

We will consider the thin annular plate shown in Fig. 2, with thickness h, and the radius of outer edge a, while its inner edge before mounting with the plate at the still state is of radius b. The plate spins at the constant angular speed ω. Let (r,φ) be a movable polar coordinate system bound to the middle area of the plate with the point of origin at the point O. The angle φ is measured starting at the line OP, which moves together with the plate.

As a result of the overlap on the inner edge of the plate being axially symmetrical, the points in the middle plate area will not move in the circular direction, i.e. only radial $u(r)$ and transversal displacements $w(r)$ will exist.

Using Karman's theory, the relationship between normal in-plane forces N_r and N_c and the displacement u is given by

$$N_r = \frac{Eh}{1-v^2}\left[\frac{\mathrm{d}u}{\mathrm{d}r} + \frac{1}{2}\left(\frac{\partial w}{\partial r}\right)^2 + v\frac{u}{r}\right],$$

$$N_c = \frac{Eh}{1-v^2}\left[\frac{u}{r} + v\frac{\mathrm{d}u}{\mathrm{d}r} + \frac{v}{2}\left(\frac{\partial w}{\partial r}\right)^2\right], \tag{1a, b}$$

where E is the Young modulus and v the Poisson ratio, whose value will be assumed to be 0.3. The squared term in Eqs. (1) will be important when examining plate stability, while it will be neglected in case of small transverse vibrations. The normal forces in the plate are given by the equation of equilibrium

$$\frac{\mathrm{d}}{\mathrm{d}r}(rN_r) - N_c + \rho h r^2\omega^2 = 0, \tag{2}$$

where ρ denotes mass per unit volume. The transverse motion of the plate is modelled using the classical Kirchhof plate theory with in-plane stresses. The governing differential equation of the motion is

$$D\nabla^4 w = -\rho h\frac{\partial^2 w}{\partial t^2} + N_r\frac{\partial^2 w}{\partial r^2} + N_c\left(\frac{1}{r}\frac{\partial w}{\partial r} + \frac{1}{r^2}\frac{\partial^2 w}{\partial \varphi^2}\right) - \rho h r\omega^2\frac{\partial w}{\partial r}, \tag{3}$$

where $D = Eh^3/12(1-v^2)$ is flexural rigidity.

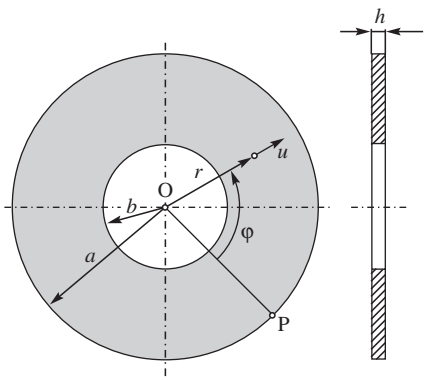

Fig. 2. Geometry of an annular plate.

The boundary conditions of the plate mounting with an overlap on the inner edge read

$$u|_{r=b} = \delta, \quad w|_{r=b} = 0, \quad \left.\frac{\partial w}{\partial r}\right|_{r=b} = 0. \tag{4a–c}$$

The boundary conditions on the outer edge in case of clamping are (see Fig. 1b)

$$u|_{r=a} = 0, \quad w|_{r=a} = 0, \quad \left.\frac{\partial w}{\partial r}\right|_{r=a} = 0, \tag{5a–c}$$

while in case of the free edge they are (see Fig. 1c)

$$N_r|_{r=a} = 0, \quad M_r|_{r=a} = 0, \quad \left.\left(Q_r - \frac{1}{r}\frac{\partial M_{rc}}{\partial \varphi}\right)\right|_{r=a} = 0, \tag{6a–c}$$

where M_r and M_{rc} denote moments, and Q_r the transversal force.

Solving the linearised equations (1) and Eq. (2) with boundary conditions (4a) and (5a), that is (4a) and (6a), normal in-plane forces will be

$$N_r = \rho h\omega^2\left(a^2 a_1 + \frac{a^4}{r^2}a_2 + a_3 r^2\right) + \frac{E\delta h}{a}\left(a_5 + \frac{a^2}{r^2}a_6\right),$$
$$N_c = \rho h\omega^2\left(a^2 a_1 - \frac{a^4}{r^2}a_2 + a_4 r^2\right) + \frac{E\delta h}{a}\left(a_5 - \frac{a^2}{r^2}a_6\right), \tag{7a, b}$$

where in case of clamping

$$a_1 = \frac{(1+k^2)(1+\nu)}{8}, \quad a_2 = \frac{k^2(1-\nu)}{8},$$
$$a_5 = -\frac{k}{(1-k^2)(1-\nu)}, \quad a_6 = -\frac{k}{(1-k^2)(1+\nu)}, \tag{8}$$

while for the free edge

$$a_1 = \frac{(1+\nu)[3+\nu+k^4(1-\nu)]}{8[1+\nu+k^2(1-\nu)]}, \quad a_2 = \frac{k^2(1-\nu)[3+\nu-k^2(1+\nu)]}{8[(1+\nu)+k^2(1-\nu)]}, \tag{9}$$

$$a_5 = \frac{k}{1+\nu+k^2(1-\nu)}, \quad a_6 = -\frac{k}{1+\nu+k^2(1-\nu)}.$$

In both cases of boundary conditions it is

$$a_3 = -\frac{3+\nu}{8}, \quad a_4 = -\frac{1+3\nu}{8}. \tag{10}$$

In all these expressions $k = b/a$.

In the case of the plate with the free outer edge the expressions for normal in-plane forces N_r and N_c, given by Eqs. (7a) and (7b), are similar to the ones obtained in Refs. [6,7] in the sense that the forms are the same but some of the coefficients are different. Due to these differences, caused by a different way of generating initial stresses, it is very difficult to compare the obtained results. Actually comparison is possible only in some special cases. In the case of the plate with the clamped outer edge, the coefficients in Eqs. (7a) and (7b) are significantly different from the ones in Refs. [6,7]; hence, it is not possible to find similarities between the results presented here and the results obtained in Refs. [6,7].

Substituting $r = b$ into Eq. (7a) and using Eqs. (9) and (10) we obtain the value of the in-plane forces N_r at the inner edge of the plate

$$N_r(b) = \rho h\omega^2 a^2\frac{1-k^2}{4} - \frac{E\delta h}{a}\frac{(1+\nu)k^2+1-\nu}{(1-k^2)k(1-\nu^2)}, \tag{11}$$

for the clamped outer edge, and

$$N_r(b) = \frac{1-k^2}{(1-\nu)k^2+1+\nu}\left[\rho h\omega^2 a^2 \frac{(1-\nu)k^2+3+\nu}{4} - \frac{E\delta h}{a}\frac{1}{k}\right], \tag{12}$$

for the free outer edge. For the sign of N_r we adopt the usual convention, meaning that the force is positive if the plate is in tension. Eqs. (11) and (12) imply that the value of N_r for small values of angular speed is negative at the inner edge of the plate. The increase of the angular speed leads to the increase of N_r and at some point N_r reaches zero. Further increases will cause the normal force N_r to become positive, which is not in agreement with the physical constraints.

In that case the plate detaches from the shaft, which results in changing boundary conditions since the plate inner edge becomes free. In order to maintain the overlap the force should meet the condition

$$N_r(b) < 0, \tag{13}$$

so the condition that the angular speed must meet is

$$\omega^2 < \frac{4\left[(1+\nu)k^2+1-\nu\right]}{(1-k^2)^2 k(1-\nu^2)}\frac{E\delta}{\rho a^3} \tag{14}$$

for the clamped outer edge, and

$$\omega^2 < \frac{4}{[3+\nu+(1-\nu)k^2]k}\frac{E\delta}{\rho a^3} \tag{15}$$

for the free outer edge. In this paper we will consider only the cases where the previously mentioned conditions are met.

After replacing Eq. (7) into Eq. (8) and introducing non-dimensional values

$$\lambda = \frac{\rho\omega^2 a^4}{Eh^2}, \quad y = \frac{w}{h}, \quad x = \frac{r}{a}, \quad \tau = t\sqrt{\frac{D}{h\rho a^4}}, \quad p = \frac{\delta a}{h^2}, \tag{16}$$

the following partial differential equation will be obtained:

$$\begin{aligned}\bar{\nabla}^4 y + \frac{\partial^2 y}{\partial \tau^2} - \eta\Bigg[&\left(\lambda a_1 + p a_5 + \frac{\lambda a_2 + p a_6}{x^2} + \lambda a_3 x^2\right)\frac{\partial^2 y}{\partial x^2} \\ &+ \left(\lambda a_1 + p a_5 - \frac{\lambda a_2 + p a_6}{x^2} + \lambda a_4 x^2\right)\left(\frac{1}{x}\frac{\partial y}{\partial x} + \frac{1}{x^2}\frac{\partial^2 y}{\partial \varphi^2}\right) - \lambda x\frac{\partial y}{\partial x}\Bigg] = 0,\end{aligned} \tag{17}$$

where $\bar{\nabla}^4 = \bar{\nabla}^2\,\bar{\nabla}^2$ is a non-dimensional biharmonic operator and $\eta = 12(1-\nu^2)$. Using non-dimensional values, the boundary conditions on the inner edge (4b,c) change into

$$y\big|_{x=k} = 0, \quad \left.\frac{\partial y}{\partial x}\right|_{x=k} = 0. \tag{18a,b}$$

Non-dimensional boundary conditions at the outer edge in case of clamping (5b,c) change into

$$y\big|_{x=1} = 0, \quad \left.\frac{\partial y}{\partial x}\right|_{x=1} = 0, \tag{19a,b}$$

while after replacing the appropriate standard expressions for moments and the force, the boundary conditions for the free edge (6b,c) will be

$$\begin{aligned}&\left(\frac{\partial^2 y}{\partial x^2} + \nu\frac{\partial y}{\partial x} + \nu\frac{\partial^2 y}{\partial \varphi^2}\right)\Bigg|_{x=1} = 0, \\ &\left[\frac{\partial^3 y}{\partial x^3} + \frac{\partial^2 y}{\partial x^2} - \frac{\partial y}{\partial x} - (3-\nu)\frac{\partial^2 y}{\partial \varphi^2} + (2-\nu)\frac{\partial^3 y}{\partial x\,\partial \varphi^2}\right]\Bigg|_{x=1} = 0.\end{aligned} \tag{20a, b}$$

The problem of determining frequencies of transverse vibration of a rotating plate with an overlap reduces to solving the partial differential equation (17) with corresponding boundary conditions.

3. Numerical solutions

The solution of Eq. (17) is obtained applying the Galerkin method. To this end, the solution is assumed in the form

$$\bar{y} = \sum_{m=0}^{M} \sum_{n=0}^{N} A_{mn} Y_{mn}(x) \cos n\varphi \sin \Omega\tau, \tag{21}$$

where A_{mn} are undetermined coefficients, M and N are the numbers of the basic functions used in the approximation, and n is the number of nodal diameters. Non-dimensional natural frequency Ω of transverse vibration is

$$\Omega = \Omega_N \sqrt{\frac{\rho h a^4}{D}}, \tag{22}$$

where Ω_N is the natural frequency and Y_{mn} are the functions chosen to satisfy the boundary conditions of the plate. They are presently assumed to be of the following form:

$$Y_{mn} = \left[1 + c_{mn}^1 x + c_{mn}^2 x^2 + c_{mn}^3 x^3 + c_{mn}^4 x^4\right] x^m, \tag{23}$$

where the constants $c_{m\,n}^s$ are chosen so that the boundary conditions are satisfied. By substituting Eqs. (21) and (23) into Eq. (17) and applying the Galerkin procedure, the following equations are obtained:

$$\sum_{m=0}^{M} A_{m\,n}(\alpha_{mnjn} - \Omega^2 \beta_{mnjn}) = 0, \quad j = 0, 1 \ldots M, \quad n = 0, 1 \ldots N, \tag{24}$$

where

$$\alpha_{mnjn} = \int_k^1 a_{mn} Y_{jn} x \, \mathrm{d}x, \quad \beta_{mnjn} = \int_k^1 Y_{mn} Y_{jn} x \, \mathrm{d}x. \tag{25a,b}$$

The expressions to be integrated in Eq. (25a) are

$$\begin{aligned} a_{mn} = {} & \frac{\mathrm{d}^4 Y_{mn}}{\mathrm{d}x^4} + \frac{2}{x}\frac{\mathrm{d}^3 Y_{mn}}{\mathrm{d}x^3} \\ & - \left[\eta(\lambda a_1 + p a_5) + \eta\lambda a_3 x^2 + \frac{1 + 2n^2 + \eta(\lambda a_2 + p a_6)}{x^2}\right] \frac{\mathrm{d}^2 Y_{mn}}{\mathrm{d}x^2} \\ & - \left[\frac{\eta(\lambda a_1 + p a_5)}{x} + \eta\lambda a_4 x - \frac{1 + \eta(\lambda a_2 + p a_6) + 2n^2}{x^3} - \lambda\eta x\right] \frac{\mathrm{d}\, Y_{mn}}{\mathrm{d}x} \\ & + \left[\frac{\eta(\lambda a_1 + p a_5)}{x^2} + \eta\lambda a_4 + \frac{n^2 - 4 - \eta(\lambda a_2 + p a_6)}{x^4}\right] n^2 \, Y_{mn}. \end{aligned} \tag{26}$$

The problem of determining transverse vibration frequencies of the plate with an overlap is reduced to solve the frequency equation representing the system of algebraic equations (24) determinant. In the rest of the paper it has been assumed that the number of assumed functions M1000 is 8 when determining frequencies.

4. Results and discussion

Figs. 3 and 4 show the first two lowest frequencies Ω, which are obtained as the lowest solutions of the frequency equation. The frequencies are shown with respect to non-dimensional angular speed λ and non-dimensional overlap p for a plate with the clamped outer edge. Doing that, it has been assumed that $k = 0.2$. The number of node diameters n changes from 0 to 3 for the first frequencies, while it assumes values 0 and 1 for the second frequencies. Bearing in mind condition (14), which determines the maximal value of angular

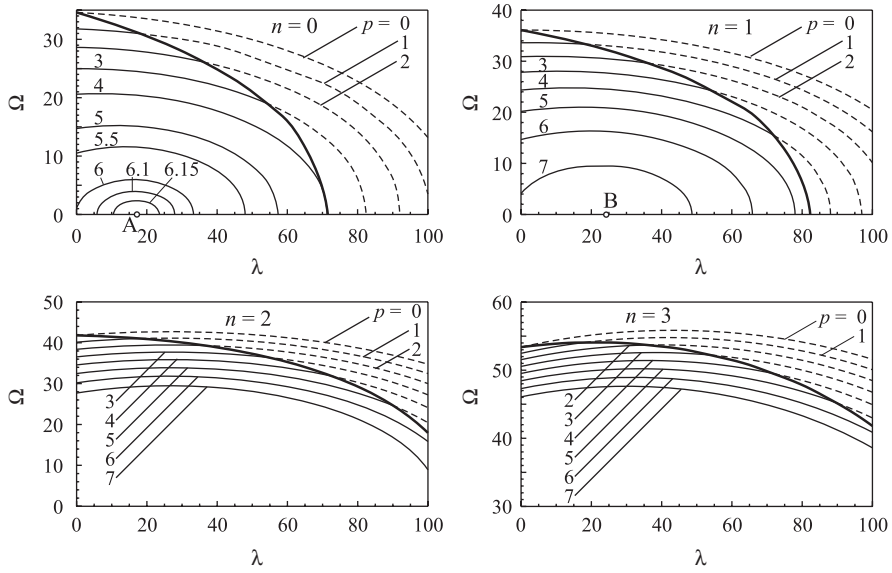

Fig. 3. The first transverse vibration frequencies of a plate with the clamped outer edge ($k = 0.2$) for different values of the number of nodes diameters n.

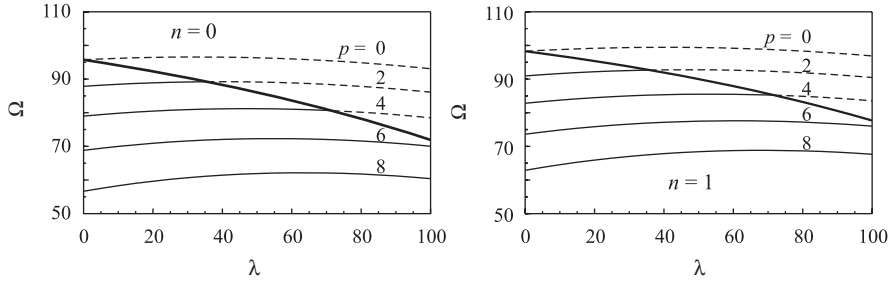

Fig. 4. The second transverse vibration frequencies of a plate with the clamped outer edge ($k = 0.2$) for different values of the number of nodes diameters n.

speed on the diagrams, the corresponding frequencies have been determined. Those frequencies are denoted by thicker lines than others on the diagrams. They intersect the frequency lines for constant values of p, and the part of the lines where the overlap has not been achieved has been denoted by a dashed line. Hence, only part of those lines denoted by a continuous line is important for consideration.

For plates with the clamped outer edge, the overlap brings about a frequency decrease. Increase of angular speed at the same overlap value influences vibration frequency change in a complex way. The diagram of frequency change at $n = 0$ given in Fig. 3 is particularly interesting. The frequency decreases with the increase of parameter λ for lower overlap values. For higher overlap values, when λ increases, vibration frequencies first increase and then decrease. If $p > 6.005$, the line of frequency change bends, forming an arc whose beginning and end are on the λ-axis. In these cases, vibration is possible only when the parameter λ is between these end points. If λ is out of this range, the frequency equation will not have the corresponding solution for Ω, that is, the lowest one will correspond to the second frequency. In case $p > 6.177$, the line of frequency change transforms into a point denoted A. Its corresponding parameter λ is $\lambda_A = 17.175$. With increase of the overlap p, vibration of the plate with the clamped edge with the first frequency and $n = 0$ is no longer possible. Point B is obtained in a similar way, where $n = 1$ and $p = 7.516$, and whose corresponding λ is $\lambda_B = 24.290$. All these frequencies are solutions of the frequency equation. But the question arises whether they are possible, because stability loss of the plate and vibration cessation may occur under the given parameters.

It is important to note that for certain λ and p values, frequencies are equal to zero, and in such cases stability loss occurs by the dynamic criterion. For $n = 0$, $p = 6.005$ there will be only one point at the right end, the frequency of which is zero for each curve. Based on this, the diagram of stability can be drawn and it is shown in Fig. 5. The diagram for $n = 1$ has been drawn in a similar way, and for higher n values these diagrams are unimportant, so they have not been shown. In order to study plate stability, it is important to determine the minimal λ value (for the p given) at which loss of stability occurs. It is obvious that the shape $n = 0$ is important for a plate with the clamped outer edge, because all minimal λ values correspond to that shape. In order to maintain the overlap, due to the limit that exists for λ parameter values, the part of the diagram that is below the limiting line, drawn thicker than other lines, is important for consideration. Because of this, the parameter area for which stability is provided is limited by this boundary line and the line $n = 0$, and that area is shaded. Hence, critical values of the parameter λ are on the line CADE, where the p and λ coordinates of points C, D and E are given by C(6.0052; 0), D(6.0052; 33.0864) and E(3.9877; 71.5130). The part of the area around point A is interesting, i.e. the area limited by the vertical line CD and the curve CD. Stability is provided for parameter values inside this area, but, if the parameter λ decreases to zero, the plate will not be stable. This means that a non-rotating plate at the overlap $p = 6$ will be unstable and that, if it starts moving so that λ is, for example, $\lambda = 20$, it will be stable. We will discuss the type of bifurcation at stability loss later.

The first two transverse vibration frequencies of a plate with the free edge, and where $k = 0.2$, are shown in Figs. 6 and 7. Similar to the case of a plate with the clamped edge, there is a limitation of the angular speed value in case of this plate too. That is why some lines are shown dashed. It is assumed that the number of nodes diameters n changes from 0 to 3 in case of the first frequency, while in case of the second it is either 0 or 1. In case of this type of boundary conditions, the transverse vibration frequency increases when the angular speed parameter increases. Besides that, in case there is an overlap, the vibration frequency will decrease, unless $n = 2$ or 3. In these exceptional cases, frequencies will increase.

At certain values of the overlap and at parameter λ, the frequency of transverse vibration is equal to zero, so stability loss occurs at these points. It can be observed in Fig. 6 that for $n = 0$, the frequency equation has a real solution when λ is greater than the critical value, and there is no solution when λ is less than the critical value. Based on this, it can be concluded that the plate will be stable if $\lambda > \lambda_{cr}$, and unstable otherwise. Fig. 8 can be produced using the data shown in all these diagrams. It shows dependence of the parameter λ on the overlap for $n = 0$ and 1, while shapes for $n > 1$ are not important. Bearing in mind that the plate is stable for $\lambda > \lambda_{cr}$, the only shape that is important for determining the critical value of λ is $n = 0$. The area of stability, which is limited by the line $n = 0$ and the boundary line of critical values of parameter λ, is shown in Fig. 8 as the shaded area. For point F, which is on the p-axis, it is given that $p = 2.3639$.

It can be noted based on the presented analyses that a plate can lose stability when it is not rotating, but is only subjected to an overlap. For that very reason the analysis of impact of an overlap on stability of a non-rotating annular plate has been performed. In Fig. 9 the critical value of the overlap p with respect to the parameter k for both cases of boundary conditions has been shown. The analysis has been performed for $n = 0$

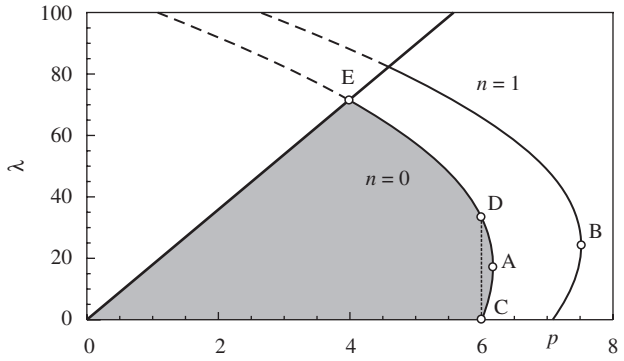

Fig. 5. Critical angular speed λ with respect to the overlap p at $k = 0.2$ in case of a plate with the clamped outer edge.

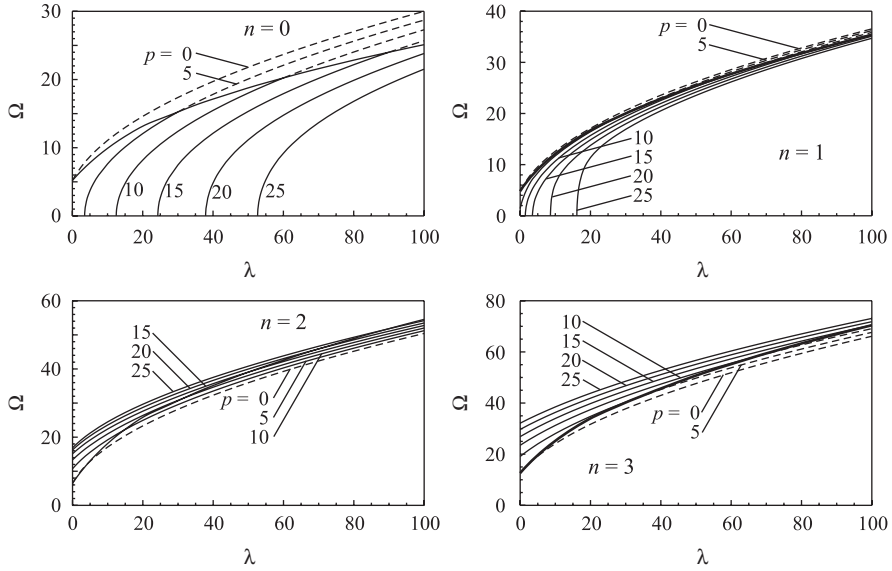

Fig. 6. The first transverse vibration frequencies of a plate with the free outer edge ($k = 0.2$) for various values of the number of nodes diameters n.

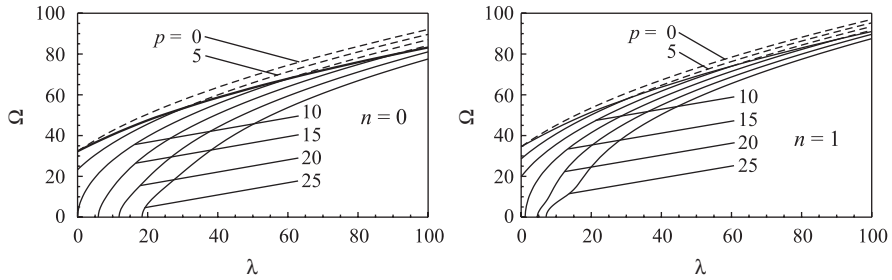

Fig. 7. The second transverse vibration frequencies of a plate with the free outer edge ($k = 0.2$) for various values of the number of nodes diameters n.

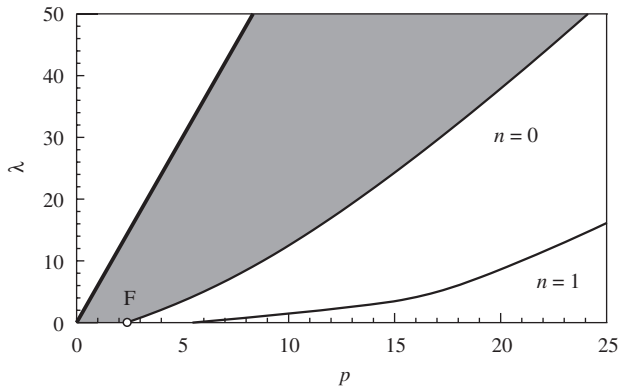

Fig. 8. The critical angular speed λ with respect to the overlap p at $k = 0.2$ in case of a plate with the free outer edge.

to 3, but in case of the free outer edge, the overlap values obtained for $n = 2$ and 3 are out of the range presented in the figure, so they have not been shown at all. It is obvious that the critical overlap value for both cases of boundary conditions are the ones that correspond to the basic shape ($n = 0$).

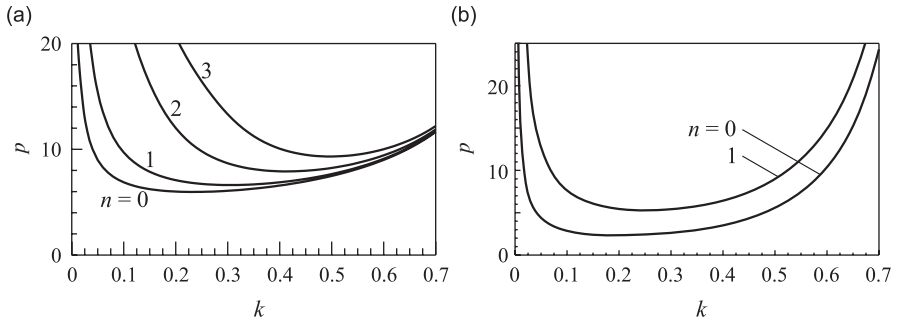

Fig. 9. The critical overlap with respect to the parameter k: (a) clamped outer edge, and (b) free outer edge.

5. Bifurcation analysis

The previous section consideration shows that linear analysis implies that loss of stability occurs when the number of nodes diameters equals zero. In this section we will perform nonlinear analysis to confirm that loss of stability really follows from linear equations and to determine the postbuckling behaviour of the plate. We will use nonlinear von Karman's equations for an axisymmetrical plate for the governing equations. As a consequence, all partial derivatives with respect to the coordinate φ are zero. Keeping this in mind, the equilibrium equation in the vertical direction reads

$$\frac{\mathrm{d}}{\mathrm{d}r}(rQ_r) = -\frac{\mathrm{d}}{\mathrm{d}r}(rN_r\theta), \tag{27}$$

where

$$\theta = -\frac{\mathrm{d}w}{\mathrm{d}r} \tag{28}$$

is the slope of the tangent in the radial direction. If we introduce the following non-dimensional quantities:

$$Q = \frac{Q_r a^3}{Eh^4}, \quad N = \frac{N_r a^2}{Eh^3}, \quad \Theta = \frac{\theta a}{h} \tag{29}$$

and integrate Eq. (27) using the boundary conditions (5c) for the plate clamped at the outer edge and Eqs. (6a,c) for the plate free at the outer edge, we get

$$Q = -N\Theta + \frac{C}{x}, \tag{30}$$

where C is a constant. In case of the plate clamped at the outer edge $C = 0$, while for the plate free at the outer edge $C = Q(1)$.

Using Eq. (30) the governing equations describing deformation of the plate can be written in the form

$$\frac{\mathrm{d}y}{\mathrm{d}x} = -\Theta, \quad \frac{\mathrm{d}\Theta}{\mathrm{d}x} = K, \quad \frac{\mathrm{d}K}{\mathrm{d}x} = -\eta N\Theta - \frac{\eta C}{x} - \frac{K}{x} + \frac{\Theta}{x^2},$$
$$\frac{\mathrm{d}N}{\mathrm{d}x} = \frac{U}{x^2} - \frac{1-\nu}{x}N - \lambda x, \quad \frac{\mathrm{d}U}{\mathrm{d}x} = (1-\nu^2)N - \frac{1}{2}\Theta^2 - \frac{\nu}{x}U, \quad \frac{\mathrm{d}C}{\mathrm{d}x} = 0, \tag{31a–f}$$

where we introduce the radial curvature k_r and the following non-dimensional parameters:

$$U = \frac{ua}{h^2}, \quad K = \frac{k_r a^2}{h}. \tag{32}$$

We note that the differential equation (31f) is not necessary in case of the plate free at the outer edge. The non-dimensional boundary conditions for the plate clamped at the outer edge are

$$U(k) = p, \quad y(k) = 0 \quad \Theta(k) = 0, \tag{33a–c}$$

at the inner edge, while at the outer edge we have

$$U(1)=0, \quad y(1)=0, \quad \Theta(1)=0. \tag{34a–c}$$

In case of the plate free at the outer edge the boundary conditions at the inner edge are given by Eqs. (33a–c), while at the outer edge they become

$$N(1)=0, \quad K(1)+v\Theta(1)=0. \tag{35a,b}$$

The trivial solution to Eqs. (31a–f) reads

$$\begin{aligned} &y_T=0, \quad \Theta_T=0, \quad K_T=0, \quad N_T=\lambda\Big(a_1+\frac{a_2}{x^2}+a_3x^2\Big)+p\Big(a_5+\frac{a_6}{x^2}\Big),\\ &U_T=\lambda\left[(1-v)a_1x-\frac{a_2}{x}(1+v)-\frac{1-v^2}{8}x^3\right]+p\left[(1-v)a_5x-\frac{1+v}{x}a_6\right], \quad C_T=0. \end{aligned} \tag{36a–f}$$

Introducing perturbations we can write the non-trivial solutions to Eqs. (31a–f) in the form

$$\begin{aligned} &y=y_T+y^*, \quad \Theta=\Theta_T+\Theta^*, \quad K=K_T+K^*,\\ &U=U_T+U^*, \quad N=N_T+N^*, \quad C=C_T+C^*. \end{aligned} \tag{37}$$

Substituting Eq. (37) into Eqs. (31) and then linearising the system obtained in this way we get the linear system that after applying the boundary conditions leads to $U_L^*=0$, $N_L^*=0$ and the following differential equation:

$$x^2\frac{\mathrm{d}^2\Theta^*}{\mathrm{d}x^2}+x\frac{\mathrm{d}\Theta^*}{\mathrm{d}x}+(b_1x^4-b_2x^2-b_3-1)\Theta^*=-\eta C^*x, \tag{38}$$

where

$$b_1=-\eta\lambda a_3, \quad b_2=\eta(\lambda a_1+pa_5), \quad b_3=\eta(\lambda a_2+pa_6). \tag{39}$$

We note that the coefficients a_i depend on the type of the supports and they are given by Eqs. (8)–(10). The general solution to Eq. (38) in case of the plate clamped at the outer edge reads (see Ref. [14])

$$\Theta_L^*=A_1\frac{1}{x}M_{\alpha,\beta}\Big(\sqrt{b_1}x^2\mathrm{i}\Big)+A_2\frac{1}{x}M_{\alpha,-\beta}\Big(\sqrt{b_1}x^2\mathrm{i}\Big)-\frac{C^*\eta}{b_3}R(x), \tag{40}$$

while in case of the free outer edge it becomes

$$\Theta_L^*=A_1\frac{1}{x}M_{\alpha,\beta}\Big(\sqrt{b_1}x^2\mathrm{i}\Big)+A_2\frac{1}{x}M_{\alpha,-\beta}\Big(\sqrt{b_1}x^2\mathrm{i}\Big). \tag{41}$$

In solutions (40) and (41) the symbol $M_{\alpha,\beta}(z)$ stands for Whittaker's function defined by

$$M_{\alpha,\beta}(z)=\mathrm{e}^{-z/2}z^{(1/2)+\beta}{}_1F_1\big(\tfrac{1}{2}+\beta-\alpha,1+2\beta,z\big), \tag{42}$$

where A_1 and A_2 are integration constants, $\mathrm{i}=\sqrt{-1}$,while the parameters α and β and the variable z are given by

$$\alpha=\frac{b_2\mathrm{i}}{4\sqrt{b_1}}, \quad \beta=\frac{1}{2}\sqrt{1+b_3}, \quad z=\sqrt{b_1}x^2\mathrm{i}, \tag{43}$$

and ${}_1F_1(\gamma,\tau,z)$ is Kummer's function defined by

$${}_1F_1(\gamma,\tau,z)=1+\sum_{n=1}^{\infty}\frac{\gamma(\gamma+1)\ldots(\gamma+n-1)z^n}{\tau(\tau+1)\ldots(\tau+n-1)n!}. \tag{44}$$

The function $R(x)$ in Eq. (40) is a particular solution to Eq. (38). We assume that $R(x)$ has a power-series representation

$$R(x)=\sum_{s=0}^{\infty}C_sx^{s+1}, \tag{45}$$

where C_s are constants to be determined. Substituting the particular solution (45) into Eq. (38) and dividing by $-C^*\eta$ we obtain

$$x^2\sum_{s=1}^{\infty}C_s(s+1)sx^{s-1}+x\sum_{s=0}^{\infty}C_s(s+1)x^s+(b_1x^4-b_2x^2-b_3-1)\sum_{s=0}^{\infty}C_sx^{s+1}=x. \tag{46}$$

From Eq. (46) it follows

$$C_0=1,\quad C_1=0,\quad C_2=\frac{b_2}{8-b_3},\quad C_3=0,\quad C_s=\frac{b_2C_{s-2}-b_1C_{s-4}}{s^2+2s-b_3}. \tag{47}$$

For the plate clamped at the outer edge solution (40) and boundary conditions (33c) and (34c) lead to

$$\Theta_L^*(k)=A_1F_1+A_2F_2-\frac{C^*\eta}{b_3}F_3=0, \tag{48a,b}$$

$$\Theta_L^*(1)=A_1F_4+A_2F_5-\frac{C^*\eta}{b_3}F_6=0,$$

where

$$F_1=\frac{1}{k}M_{\alpha,\beta}(\sqrt{b_1}k^2\mathrm{i}),\quad F_2=\frac{1}{k}M_{\alpha,-\beta}(\sqrt{b_1}k^2\mathrm{i}),\quad F_3=R(k), \tag{49}$$

$$F_4=M_{\alpha,\beta}(\sqrt{b_1}\mathrm{i}),\quad F_5=M_{\alpha,-\beta}(\sqrt{b_1}\mathrm{i}),\quad F_6=R(1).$$

Integrating Eq. (31a) and then using the boundary conditions (33b) and (34b) we have

$$y_L^*(k)-y_L^*(1)=\int_k^1\Theta_L^*\,\mathrm{d}x=0. \tag{50}$$

Next, we substitute the general solution given by Eq. (40) into Eq. (50) to obtain

$$A_1F_7+A_2F_8-\frac{C^*\eta}{b_3}F_9=0, \tag{51}$$

where

$$F_7=\int_k^1\frac{1}{x}M_{\alpha,\beta}(\sqrt{b_1}x^2\mathrm{i})\,\mathrm{d}x,\quad F_8=\int_k^1\frac{1}{x}M_{\alpha,-\beta}(\sqrt{b_1}x^2\mathrm{i})\,\mathrm{d}x,\ F_9=\int_k^1R(x)\,\mathrm{d}x. \tag{52}$$

Using Eqs. (48a), (48b) and (51) we obtain the characteristic equation

$$F_1(F_5F_9-F_6F_8)+F_2(F_6F_7-F_4F_9)+F_3(F_4F_8-F_5F_7)=0. \tag{53}$$

Now solution (40) becomes

$$\Theta_L^*=A_1\mathrm{Re}\left[\frac{1}{x}M_{\alpha,\beta}(\sqrt{b_1}x^2\mathrm{i})+\frac{F_3F_4-F_1F_6}{F_2F_6-F_3F_5}\frac{1}{x}M_{\alpha,-\beta}(\sqrt{b_1}x^2\mathrm{i})+\frac{F_1F_5-F_4F_2}{F_2F_6-F_3F_5}R(x)\right]. \tag{54}$$

In the case of the plate free at the outer edge it follows from the general solution (41) and the boundary condition (33c) that

$$\Theta_L^*(k)=A_1G_1+A_2G_2=0, \tag{55}$$

where

$$G_1=M_{\alpha,\beta}(\sqrt{b_1}k^2\mathrm{i}),\quad G_2=M_{\alpha,-\beta}(\sqrt{b_1}k^2\mathrm{i}). \tag{56}$$

Using Eq. (31b) the boundary condition (35b) becomes

$$\frac{\mathrm{d}}{\mathrm{d}x}\Theta_L^*(1)+\nu\Theta_L^*(1)=0. \tag{57}$$

We note that the derivative of Whittaker's function reads as follows (see Ref. [15, Eq. (13.4.32)])

$$\frac{\mathrm{d}M_{\alpha,\beta}(z)}{\mathrm{d}z}=\frac{1}{z}\left(\frac{1}{2}z-\alpha\right)M_{\alpha,\beta}(z)+\frac{1}{z}\left(\frac{1}{2}+\beta+\alpha\right)M_{\alpha+1,\beta}(z). \tag{58}$$

Since the derivative of $M_{\alpha,\beta}(z)$ with respect to x is

$$\frac{\mathrm{d}M_{\alpha,\beta}(z)}{\mathrm{d}x}=\frac{\mathrm{d}M_{\alpha,\beta}(z)}{\mathrm{d}z}2\sqrt{b_1}\mathrm{i}x, \tag{59}$$

from solution (41) and boundary condition (57) it is seen that

$$A_1G_3+A_2G_4=0, \tag{60}$$

where

$$G_3=(\sqrt{b_1}\mathrm{i}-2\alpha-1+v)M_{\alpha,\beta}(\sqrt{b_1}\mathrm{i})+(1+2\beta+2\alpha)M_{\alpha+1,\beta}(\sqrt{b_1}\mathrm{i}), \tag{61}$$

$$G_4=(\sqrt{b_1}\mathrm{i}-2\alpha-1+v)M_{\alpha,-\beta}(\sqrt{b_1}\mathrm{i})+(1-2\beta+2\alpha)M_{\alpha+1,-\beta}(\sqrt{b_1}\mathrm{i}).$$

Eqs. (55) and (60) lead to the following characteristic equation:

$$G_1G_4-G_2G_3=0. \tag{62}$$

The angle of the tangent in the radial direction now becomes

$$\Theta_L^*=A_1\frac{1}{x}\mathrm{Re}[M_{\alpha,\beta}(\sqrt{b_1}x^2\mathrm{i})-\frac{G_1}{G_2}M_{\alpha,-\beta}(\sqrt{b_1}x^2\mathrm{i})]. \tag{63}$$

By integrating Eq. (31a) with use of expression (54) or (63), as well as the boundary condition (33b), the shape of the plate at stability loss can be obtained.

Solving the characteristic equations (53) and (62) we obtain the critical values of the parameter λ. In Tables 1 and 2 we compared these values to the ones calculated by using the Approximate Galerkin method in the third section. From these tables one can conclude that the agreement between the results is quite satisfactory for greater values of k and lower values of p.

In the following paragraphs we apply the Liapunov–Schmidt procedure to investigate the postbuckling behaviour of the plate. A detailed description of the procedure along with examples is given in Ref. [16, Chapter VII] or Ref. [17, pp. 30–34]. Due to the complexity of the expressions resulting from applying the procedure, we skip the intermediate steps and give only the final result, i.e. the following algebraic bifurcation equation:

$$g(\bar{a},\lambda_{cr}+\Delta\lambda)=c_1\bar{a}\Delta\lambda+c_3\bar{a}^3+O(|\bar{a}|^2\Delta\lambda,|\bar{a}|^4), \tag{64}$$

where $\Delta\lambda\ll1$ is perturbation of the critical load, $\bar{a}$ is a small real amplitude parameter (see Ref. [16], or Ref. [18]) and c_1, c_3 are coefficients to be calculated. The formal form of the coefficients c_1 and c_3 is presented

Table 1
Comparing the critical values of parameter λ obtained by Galerkin method to ones calculated from Eq. (53) for the plate clamped at the outer edge

K	p	Galerkin (24)	Eq. (53)
0.1	4	64.35909	64.35907
	5	57.41189	57.41183
	6	48.50836	48.50795
0.2	4	71.36364	71.36364
	5	57.39411	57.39411
	6	33.31625	33.31622

Table 2
Comparing the critical values of parameter λ obtained by Galerkin method to ones calculated from Eq. (62) for the plate free at the outer edge

k	p	Galerkin (24)	Eq. (62)
	4	1.21041	1.21042
0.1	5	2.54244	2.54250
	6	4.18134	4.18154
	4	2.07111	2.07111
0.2	5	3.47986	3.47987
	6	5.01303	5.01303

by Eqs. 3.23(c) and 3.23(e) on p. 33 of Ref. [16]. In the case investigated here the coefficient c_1 is given by

$$c_1 = \int_k^1 \left(a_1 x + \frac{a_2}{x} + a_3 x^3\right)(\Theta_L^*)^2 \, \mathrm{d}x. \tag{65}$$

The coefficient c_3 reads

$$c_3 = \frac{1}{2}\int_k^1 N_2 x(\Theta_L^*)^2 \, \mathrm{d}x, \tag{66}$$

where N_2 follows from the following differential equations (see Ref. [16, Eq. (3.22a) on p. 33]):

$$\frac{\mathrm{d}N_2}{\mathrm{d}x} = \frac{U_2}{x^2} - \frac{1-\nu}{x}N_2, \quad \frac{\mathrm{d}U_2}{\mathrm{d}x} = (1-\nu^2)N_2 - \frac{\nu}{x}U_2 - (\Theta_L^*)^2. \tag{67}$$

The boundary conditions corresponding to Eqs. (67) in the case of the plate clamped at the outer edge is

$$U_2(k) = 0, \quad U_2(1) = 0, \tag{68}$$

while in case of the plate free at the outer edge they become

$$U_2(k) = 0, \quad N_2(1) = 0. \tag{69}$$

We note systems (66)–(69) are equivalent to the one given by Eqs. (67)–(69) and

$$\frac{\mathrm{d}\zeta}{\mathrm{d}x} = \frac{1}{2}N_2 x(\Theta_L^*)^2, \tag{70}$$

subject to

$$\zeta(k) = 0, \tag{71}$$

where the dependent variable ζ satisfies $c_3 = \zeta(1)$. In the calculations system (67)–(71) is used to calculate the coefficient c_3.

Next we study the qualitative behaviour of the solution. Thus according to Keyfitz [19] we can neglect the higher order terms in Eq. (64) and conclude that this equation is contact equivalent to

$$g(\bar{a}, \lambda_{\mathrm{cr}} + \Delta\lambda) = \mathrm{sgn}(c_1)\bar{a}\Delta\lambda + \mathrm{sgn}(c_3)\bar{a}^3. \tag{72}$$

Therefore, Eq. (64) has a pitchfork bifurcation and the type of bifurcation depends on the sign of the coefficients c_1 and c_3. If the constants c_1 and c_3 are of the same sign, the bifurcation is called subcritical, while in the case when they are of the opposite sign, the bifurcation is supercritical.

Now we analyse the value of coefficients c_1 and c_3 in case of the plate clamped at the outer edge. For $k = 0.2$ the stability boundary is presented in Fig. 5. After calculating the values of c_1 and c_3 along the stability boundary, we find that $c_1 > 0$ and $c_3 > 0$ between the points C and A, so that bifurcation is subcritical. Next, we calculate the values of c_1 and c_3 between points A and E and get $c_1 < 0$ and $c_3 > 0$. This means that the bifurcation is supercritical. At point A we have $c_1 = 0$ and $c_3 > 0$, so the higher order terms in the bifurcation equation (64) are needed if the type of bifurcation is to be determined.

The stability boundary of the plate free at the outer edge is shown in Fig. 8 and it is calculated for $k = 0.2$. Calculations show that both coefficients c_1 and c_3 are positive all the way along the stability boundary, so bifurcation is subcritical.

Concluding this section we can point out that the smallest positive roots of Eqs. (53) and (62) determine bifurcation points and represent the critical angular speed λ_{cr} for the plate clamped at the outer edge and the plate free at the outer edge, respectively.

6. Postcritical behaviour of an annular plate with an overlap

In order to obtain the postcritical shape of the plate, we numerically integrate the nonlinear system of differential equations (31). For the plate clamped at the outer edge and $k = 0.2$, the non-dimensional deflection at $x = 0.6$ against the angular velocity λ is presented in Fig. 10a. The values of an overlap p used to obtain diagrams are 6, 6.1, 6.17755 and 6.23.

For $p = 6$ it can be noted that an increase of λ leads to an increase of deflection; hence the bifurcation is supercrtitical. When $p = 6.1$, there are two curves in Fig. 10a. The first of them, corresponding to smaller values of λ, μ shows that an increase of λ leads to a decrease of deflection, which implies the occurrence of subcritical bifurcation. The second curve corresponds to the larger values of λ and leads to supercritical bifurcation. Therefore, for $p = 6.1$ there are two critical values of λ, upper and lower, so that the plate remains stable when λ takes values between them. By increasing the overlap the distance between the critical values of λ is getting smaller and for $p = 6.17755$ it disappears. It has been shown that at this value of the overlap the parameter c_1 is $c_1 = 0$. By increasing the overlap further to $p = 6.23$, the plate becomes unstable for each value of λ.

By taking $p = 6.1$ the different buckled shapes of the plate are shown in Fig. 10b. The dashed line represents subcritical, while the full line represents supercritical buckled shapes. It can be seen that increase in angular

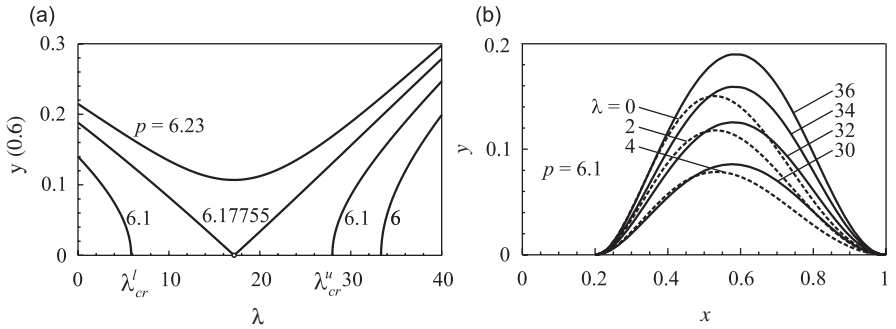

Fig. 10. Postcritical behaviour of the plate clamped at the outer edge ($k = 0.2$): (a) deflection at $x = 0.6$ with respect to λ and certain values of overlap p, and (b) postcritical shape for $p = 6.1$.

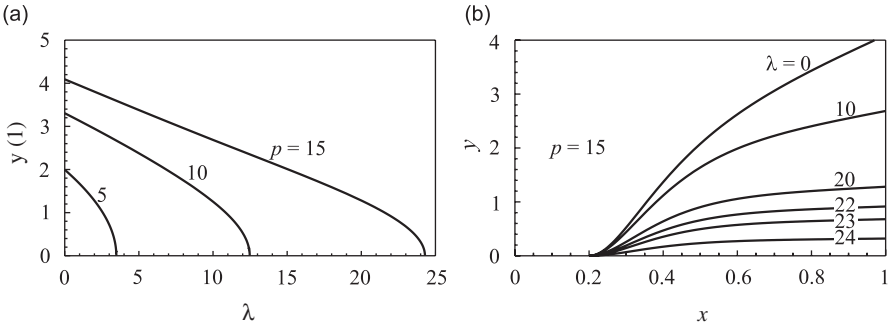

Fig. 11. Postbuckling behaviour of the plate free at the outer edge ($k = 0.2$): (a) deflection at the outer edge with respect to λ and certain values of overlap p, and (b) postcritical shape for $p = 15$.

velocity causes the place of maximum deflection to get further and further away from the centre of the plate. These results are in agreement with the results obtained by using the dynamic method of stability analysis presented in Sections 3 and 4 and the results obtained by using the adjacent equilibrium method for stability analysis presented in Section 5.

For the plate free at the outer edge we integrate numerically the nonlinear system (31) by taking $k = 0.2$ to determine deflection at the outer edge. The relation between this deflection and the angular velocity is shown in Fig. 11a for p taking the values 5, 10 and 15. From this figure it follows that for all values of p deflection at the outer edge of the plate decreases as angular velocity increases. By assuming the value $p = 15$, the different shapes of the plate after losing stability are shown in the Fig. 11b. This case also shows that plate displacements are greater when it does not rotate ($\lambda = 0$), than when it does (for example, at $\lambda = 20$), which implies subcritical stability loss, as was mentioned earlier.

7. Conclusions

1. Mounting of a rotating plate with an overlap can have great influence on lateral vibration frequencies. It is shown that an overlap influences vibration frequencies in a very complex way, and depending on the number of nodes diameters can increase or decrease in frequencies. In the vibration mode with no nodal diameters an overlap at the inner edge of the plate decreases vibration frequency. Thus in this case the influence of an overlap is similar to the influence of the thermal effect in Refs. [6,13] or to initial in-plane stresses [6,7].
2. A plate mounted with an overlap can loose stability. For both boundary conditions and for all values of the parameter k loss of stability occurs in the mode with no nodal diameters. The stability boundary is determined in two different ways. In the first case the Galerkin method is used while in the second case the stability boundary followed from the linearised governing equations. The analytical solution to the linearised governing equations is expressed in terms of Whittaker's function. It is also shown that both ways lead to the same stability boundary.
3. In the case of the plate clamped at the outer edge, bifurcation can be both supercritical and subcritical depending on the values of parameters. However, the postbuckling analysis of a plate free at the outer edge shows that only subcritical bifurcation is possible.
4. For certain values of angular velocity it is possible to achieve increase of values of critical overlap that causes stability loss compared with the plate that does not rotate. Therefore, in these cases rotation can be used to stabilise the plate.
5. We want to mention one possible way to generalise the problem presented here. Namely, we think that it could be very interesting to treat this problem by taking an elastic shaft instead of the rigid one in order to find out how elasticity influences the stability boundary.

Acknowledgements

This research was supported by the Ministry of Science, Technologies and Development of Republic of Serbia.

References

[1] H. Lamb, R.V. Southwell, The vibrations of a spinning disk, *Proceedings of the Royal Society of London* 99 (1921) 272–280.
[2] R.V. Southwell, On the free transverse vibration of a uniform circular disk clamped at its center and on the effects of rotation, *Proceedings of the Royal Society of London* 101 (1922) 133–153.
[3] S. Barasch, Y. Chen, On the vibration of a rotating disk, *ASME Journal of Applied Mechanics* 39 (1972) 1143–1144.
[4] G.K. Ramaian, Natural frequencies of spinning annular plates, *Journal of Sound and Vibration* 74 (1981) 303–310.
[5] W. Eversman, R.O. Dodson, Free vibration of a centrally clamped spinning circular disk, *American Institute of Aeronautics and Astronautics Journal* 7 (1969) 2010–2012.
[6] C.D. Mote, Free vibration of initially stressed circular disks, *ASME Journal of Engineering for Industry* 87B (1965) 258–264.
[7] G.S. Schajer, C.D. Mote Jr., Analysis of roll tensioning and its influence on circular saw stability, *Wood Science and Technology* 17 (1983) 287–302.

[8] R. Maretic, Vibration and stability of rotating plates with elastic edge supports, *Journal of Sound and Vibration* 210 (1998) 291–294.
[9] H. Ouyang, J.E. Mottershead, A bounded region of disc-brake vibration instability, *ASME Journal of Vibration and Acoustics* 123 (2001) 543–545.
[10] J.H. Wolkowisky, Existence of buckled states of circular plates, *Communications on Pure and Applied Mathematics* XX (1967) 546–560.
[11] A.K. Machinek, H. Troger, Postbuckling of elastic annular plates at multiple eigenvalues, *Dynamics and Stability of Systems* 3 (1988) 78–98.
[12] K.K. Raju, G.V. Rao, Postbuckling analysis of moderately thick elastic circular plates, *ASME Journal of Applied Mechanics* 50 (1983) 468–470.
[13] R.B. Maretic, V.B. Glavardanov, Stability of a rotating heated circular plate with elastic edge support, *ASME Journal of Applied Mechanics* 71 (2004) 896–899.
[14] E. Kamke, *A Handbook of Ordinary Differential Equations*, Nauka, Moscow, 1976 (in Russian).
[15] M. Abramowitz, I. Stegun, *Handbook of Mathematical Functions*, Dower Publications, New York, 1965.
[16] M. Golubitsky, D.G. Scaeffer, *Singularities and Groups in Bifurcation Theory*, Vol. 1, Springer, New York, 1985.
[17] S.N. Chow, J.K. Hale, *Methods of Bifurcation Theory*, Springer, New York, 1982.
[18] H. Troger, A. Steindl, *Nonlinear Stability and Bifurcation Theory: An Introduction for Engineers and Applied Scientists*, Springer, Wien, 1981.
[19] B.L. Keyfitz, Classification of one-state variable bifurcation problems up to codimension seven, *Dynamics and Stability of Systems* 1 (1986) 1–41.